Alcazar-Ruiz *et al. Chem. Biol. Technol. Agric.* (2023) 10:56
https://doi.org/10.1186/s40538-023-00431-6

Chemical and Biological Technologies in Agriculture

RESEARCH

Open Access

Hydrocarbon selectivity enhancement through catalytic fast co-pyrolysis of almond shell and plastic blends

A. Alcazar-Ruiz[1], L. Sanchez-Silva[1*] and F. Dorado[1]

Abstract

Background The aim of this article is to explore possible pathways for the synergistic optimization of bio-oil by the catalytic fast co-pyrolysis of almond shell (AS) and plastic residues (polyethylene, PE, and polystyrene, PS). Pyrolysis was carried out at 650 °C at a heating rate of 20 °C/ms at a residence time of 20 s. Hydrogen from the plastic promoted the decarboxylation of acids and decarbonylation of carbonyls and sugars from biomass waste.

Results Co-pyrolysis results showed a fall in oxygen in the AS/plastics blends, whereas carbon yields increased as did the calorific value of the oil. As expected, AS/PE blends enhanced production of hydrocarbon fractions, especially olefins, with yields reaching 81.1%, whereas AS/PS blends enhanced formation of aromatic compounds. HZSM-5 assisted the increase of monocyclic aromatics content in AS/PE blends. AS/PS blends favoured the increased of aromatics (45% of total hydrocarbons for 1:2 AS/PE-HZ). For AS/PS-HZ blends toluene was enhanced as was the production of 1,3,5-cycloheptatriene.

Conclusions These findings helped to gain a great insight into how catalytic co-fast pyrolysis of feedstocks can enhance the formation of value-added products, promoting their economic potential for agricultural exploitations.

Keywords Almond shell, Catalytic co-fast pyrolysis, Hydrocarbon selectivity, Polyethylene, Polystyrene, Aromatics

*Correspondence:
L. Sanchez-Silva
marialuz.sanchez@uclm.es
Full list of author information is available at the end of the article

Graphical Abstract

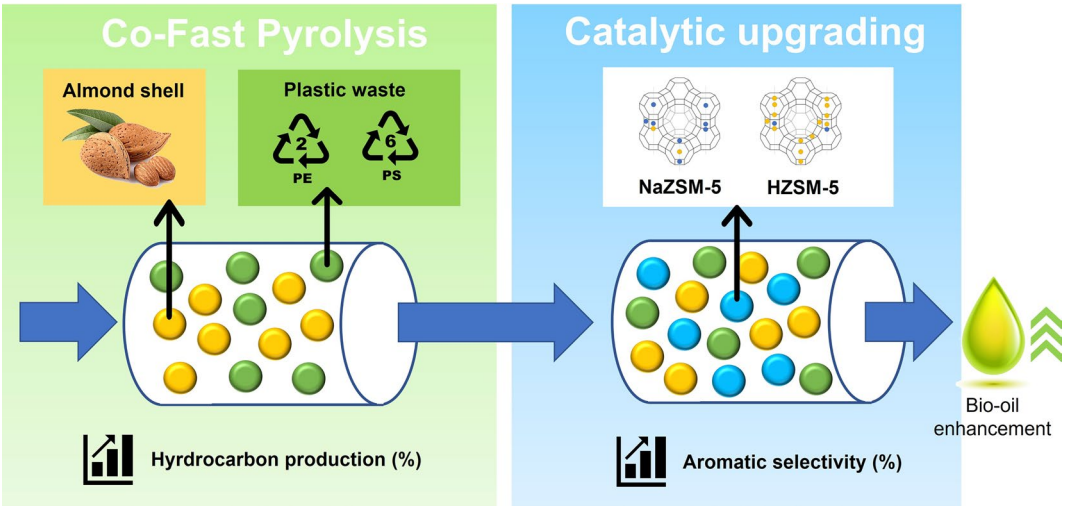

Background

Climate change and energy crises caused by dependence on fossil fuels are a constant concern. Against this backdrop, harnessing renewable energy sources that can easily be replenished should be evaluated easily [1]. The use of biomass as a promising option for thermochemical conversion has gained interest due to the production and disposal rates of various residues. Nut shells, in particular, have caught attention not only for their abundant production but also for their internal chemical composition [2]. Almond shells, for instance, are biodegradable residues from the processing of almonds [3], the most abundant crop worldwide in the 2020/2021 harvest, with 1.7 million metric tons of kernels produced [4]. Currently, almond shells are either discarded or used for livestock bedding, dairy feed, and electricity generation through combustion. Thermochemical conversion of almond shells is a beneficial alternative to produce value-added products such as biofuels, bio-chemical chains, and functional biocarbon materials [5–7].

Different thermochemical methods such as pyrolysis offer one possible solution. Fast pyrolysis leads to high bio-oil yields (approximately 75 wt%) and occurs at high heating rates, moderate temperatures, and short residence times [8]. One possible option for use as an abundant, renewable feedstock in fast pyrolysis is lignocellulosic biomass which contains aromatic hydrocarbons [9]. However, its hydrogen-deficient nature results in undesirable features in the bio-oil properties: low calorific value, high viscosity, and thermal instability. This is because it consists of a mixture of oxygenated compounds (acids, phenols and short chain oxygen compounds) and as such it is of limited use in industry [10]. Therefore, one simple way of producing high yields of bio-oil of better quality is to use hydrogen-rich material in co-pyrolysis. One solution put forward by Sut et al. [11] was to add hydrogen-rich solid wastes (such as plastics) to the biomass in co-pyrolysis to promote decarboxylation and decarbonylation. In these processes, acids and other oxygenated organic compounds in the bio-oil are removed, thus increasing its calorific value. Furthermore, plastic waste is presented herein as a solid feedstock. It can be blended with lignocellulosic biomass residues, which would raise its financial and environmental value. Abnisa et al. found yields rose from 46.1 to 61.3 wt% on adding polystyrene (PS) to palm shells [12]. Yang et al. investigated the co-pyrolysis of low-density polyethylene (LDPE) with three types of biomasses and found that the inorganic elements in the biomass facilitated the decomposition of LDPE. However, they observed an increase in larger organic molecules (>C12) due to the reaction between the decomposition products of LDPE and biomass [13]. Al-Maari et al. studied the co-pyrolysis of biomass wastes with polyethylene (PE). They had a positive synergistic effect on the formation of aliphatic hydrocarbons and overall all feedstocks decreased the amount of oxygenated compounds in this potential fuel substitute [14]. Van Nguyen et al. demonstrated that the water content and acetic acid concentration decreased as the hydrocarbon production increased in the obtained bio-crude oil from the co-pyrolysis of pine sawdust and PS [15]. However, co-pyrolysis improves oil quality, since the synergistic effects enhance oil stability, promote

hydrocarbon formation and reduce reactive oxygenates compounds [16]. Furthermore, unprecedented growth in mixed plastic and biomass wastes such as plastic bags, drinking water bottles, agro- and forestry-waste, along with COVID-19 driven waste have obliged the scientific community to look for technologies that can process and convert both biomass and plastic wastes together into useful end-products [17].

To upgrade the oil from co-pyrolysis, it must first be subjected to a catalyst. For this purpose, efficient catalysts are used for reducing oxygen content and heavy hydrocarbons [18]. Catalysts may be added in co-pyrolysis and oxygen is removed via decarboxylation, dehydration and decarbonylation which results in upgraded bio-oil. Traditional zeolites vary in porosity and acidity which may influence their cracking catalytic effect in biomass pyrolysis [19]. Among these, protonic type Zeolite Socony Mobil-5 (HZSM-5) is the most active deoxygenation catalyst. It has high selectivity in terms of producing aromatic hydrocarbons such as BTX (benzene, toluene and xylene) and PAHs (polycyclic aromatic hydrocarbons) [20]. Lazaridis et al. found that phenol branches can easily be removed with Brønsted acids and transformed into olefins (ethylene, propylene). These could directly form monocyclic aromatic hydrocarbons through aromatization [21]. Lin et al. reported a synergistic increase in yields of aromatics and valuable mono-aromatic selectivity during the catalytic co-pyrolysis of corn stover and waste plastic with a HZSM-5 zeolite [22]. However, Dyer et al. investigated the effect of zeolite ZSM-5 impregnated with different metals on the co-pyrolysis of biomass and waste PS. The results showed that the different added metals had a different impact on the yield, deoxygenation pathways, and composition of the product oils and gases [23]. This study used plastics and biomass wastes in equal measure. In other words, the biomass content was changed from 100 to 0% in the blends and the same was performed for plastics, although this marked a digression from the goal of using renewable biomass sources. Moreover, using a common catalyst (and modified versions of it) to upgrade fast-pyrolysis bio-oil by reducing the oxygen in it incurs additional expenses or large changes to operating conditions [24].

In this study, almond shell as the oxygen-rich biomass waste, polyethylene (PE) and polystyrene (PS) were used as hydrogen donors. Its aim was to research what effect catalytic fast co-pyrolysis had on the selectivity of hydrocarbon products, and to enhance production of value-added compounds, such as benzene, toluene and xylene (BTX). The catalytic effect of zeolites on yield and the composition of the bio-oil produced is compared and discussed. Furthermore, the joint effect of inherent alkali and alkaline earth metals (AAEMs) in the biomass and adding zeolite to the yields of aromatics is evaluated.

Methods

Feedstock samples

In this paper, an agricultural biomass residue, almond shell (AS), collected in Castilla-La Mancha (Spain) was mixed with polyethylene (PE) and polystyrene (PS)—both typical agricultural plastic wastes—and underwent catalytic fast co-pyrolysis. Beforehand, the samples were oven-dried for 24 h at 100 °C, milled and sieved. An average particle size ranging from 100 to 150 μm was obtained. PE and PS were purchased from Sigma-Aldrich, ground and sieved to a particle size under 0.1 mm.

Table 1 Feedstock characteristic data analysis

Sample	Proximate analysis (wt%)*^{daf}				Ultimate analysis (wt%)*^{daf}				HHV (MJ/kg)	H/C_{eff}
	Moisture	Ash	Volatile matter	Fixed carbon*^{diff}	C	H	N	O*^{diff}		
AS	3.11	4.24	78.48	14.16	47.21	5.71	0.45	46.6	18.3	0.3
PE	0.45	0.22	99.27	0.06	85.70	14.20	0.05	0.05	46.63	1.98
PS	0.26	2.39	97.30	0.04	92.31	7.72	0	0	41.27	1.01
	Mineral content (wt%)									
	Ca	K	Mg	Na						
AS	0.29	1.16	0.032	0.058						
	Chemical composition (wt%)^{db}									
	Lignin	Cellulose	Hemicellulose							
AS	13.4	28.1	39.7							

daf: dry and ash free basis; O^{diff}: % of oxygen calculated from the difference in C, H, and N; fixed carbon*diff: % in fixed carbon calculated from difference in moisture, ash and volatile matter; *db: dry basis

Sample characterization

An ultimate and proximate analysis were carried out according to UNE 15104:2011, UNE-EN ISO18123:2016, UNE 32-004-84 and UNE 32-002-95 standards in a Thermo Fischer Scientific Flash 2000 elemental analyser, equipped with a thermal conductivity detector. The proximate analysis provided data on moisture, ash, volatile matter and fixed carbon content. Also, an ultimate analysis was carried out to find the concentrations of carbon, hydrogen, nitrogen, oxygen and sulphur in the sample. In addition, metal content was determined by inductively coupled plasma-optical emission spectrometry (ICP-OES) with Varian 720-ES equipment (previously calibrated using an ICP multi-element standard solution IV, Merck).

From the ultimate analysis, the hydrogen-to-carbon effective molar ratio (H/C_{eff}) was determined with the following equation (Eq. 2) [25]:

$$H/C_{\text{eff}} = \frac{H - 2 \cdot O - 3 \cdot N - 2 \cdot S}{C}, \quad (1)$$

where H, C, O and N are the moles of hydrogen, carbon, oxygen and nitrogen.

The higher heating value (HHV) shown in Table 1 was calculated from the elemental analysis based on the ultimate data analysis with the following empirical correlation (Eq. 1) [26]:

$$\text{HHV}\left(\frac{\text{MJ}}{\text{kg}}\right) = 0.3491 \cdot C + 1.1783 \cdot H + 0.1005 \cdot S - 0.1034 \cdot O - 0.0151 \cdot N - 0.0211 \cdot A, \quad (2)$$

where C, H, S, O, N and A are the weight percentages of carbon, hydrogen, sulphur, oxygen, nitrogen, and ash, respectively.

For AS, lignin, hemicellulose and cellulose content were calculated with an experimental methodology reported by López-González et al. [27]. Solvent extraction (100 ml acetone for 1 g of dried biomass sample) at 60 °C was used to determine the amount of extractives. Then, the sample was dried at 110 °C until the weight was constant. The solid residue was then cooled to room temperature and weighed. The weight difference before and after extraction equalled the quantity of extractives. For determining hemicellulose content, 150 ml of NaOH (20 g l^{-1}) was added to 1 g of extractive-free material and boiled for 3.5 h with recycled water. Next, it was filtered and repeatedly washed until all Na^+ had been removed and dried at 110 °C for 1 h. The difference in weight after treatment determined the amount of hemicellulose. Regarding the quantity of lignin, this was assessed using the Klason method (TAPPI T 222 om-02) [28]. The sample of extractive-free material was then added to 3 ml of H_2SO_4 (72%) at 30 °C for 1 h and diluted to 3% w/w H_2SO_4. The resulting mixture was boiled for 4 h with recycled water. After that, the residue was filtered, washed and dried. Once again, the difference in weight accounted for the lignin. Finally, the amount of cellulose was calculated by the differences in weight in extractives, hemicellulose, and lignin. The results are given in Table 1.

Thermogravimetric characterization

Thermogravimetric analysis (TGA) and the corresponding differential thermogravimetric analysis (DTG) were carried out in a TGA apparatus (TGA 2, Mettler Toledo). The experiments were performed at temperatures ranging from 25 to 1000 °C at a heating rate of 10 °C min^{-1} and a constant flow of 90 ml min^{-1} under an inert atmosphere (N_2). The initial sample weight was fixed at 20 mg, each of which was analysed at least three times and average values were recorded. The experimental standard deviation was ±0 0.5% in weight loss and ±2 °C in temperature.

Table 2 Characterization data of NaZSM-5 and HZSM-5

Sample	NaZSM-5	HZSM-5
S_{BET} (m^2/g)	437	441
Total acidity (mmol NH_3/g)	0.39	0.61
Weak acid (mmol NH_3/g)	0.39	0.02
T desorption (°C)		295
Strong acid (mmol NH_3/g)	0.00	0.59
T desorption (°C)		400

Catalyst preparation

The zeolite ZSM-5 was supplied in ammonium form by Zeolyst International (Si/Al = 25). In order to change it to protonic form HZSM-5, it was calcined at 550 °C for 15 h and the sodium form NaZSM-5 was obtained by ion-exchange with 5 M $NaNO_3$ (35 ml g^{-1}). Next, the slurry was filtered, washed with deionized water, dried at 110 °C and left overnight. This procedure was repeated three times after which the sample was calcined for 4 h at 550 °C. Total sodium content in NaZSM-5 (determined by atomic absorption spectrophotometry using a Spectra 220FS analyzer) was 2.04 wt%

The surface area for BET was found by calculating the adsorption and desorption data acquired with a Micromeritics ASAP 2010 apparatus. Then, the degree to which acid sites were concentrated was found by a

temperature-programmed desorption of ammonia using a Micromeritics TPD/TPR analyzer. For further details on both techniques, see Dorado et al. [29]. The results are given in Table 2.

Catalytic co-pyrolysis procedure analysis

The catalytic fast co-pyrolysis tests for AS mixed with PE and PS were performed in a Py-GC/MS (CDS Pyroprobe 6200 g and Agilent Technologies 7890B/5977B GC/MS).

In different experiments biomass and plastic wastes (PE and PS) were mixed. The ratio of AS to plastic was optimized as in a previous study [30] which was 1.5:1 for AS/PE and 1:1.5 for AS/PS blends. To study the catalytic effect, zeolites were blended with the biomass–plastic mixture by varying the biomass/plastic–zeolite mass ratio (2:1, 1:1 and 1:2). Here, sample 1:2 AS/PS-HZ was a mixture of almond shell/polystyrene (1:1.5 AS/PS) and HZSM-5 (HZ) zeolite in a ratio of 1:2. In all the experiments the total feedstock mass was kept at 1 mg ± 0.05 mg and placed in the middle of a quartz tube (2 mm diameter and 20 mm long) with a quartz wool base. The sample was weighed on an analytical balance at an accuracy of 0.001 mg (XSR105DU, Mettler-Toledo, Switzerland). Fast pyrolysis was conducted at 650 °C at a heating rate of 20 °C ms^{-1} at a residence time of 20 s. These operational conditions as well as the ratio of biomass/plastic mass had been optimized in previous research [30].

For the analysis, the GC/MS injector temperature was kept at 280 °C. An Elite-35MS capillary column (30 m × 0.25 μm) was used for chromatographic separation. Helium (99.999%) was used as the carrier gas at a constant flow rate of 1 ml min^{-1} with a 1:80 split ratio which enabled the chemicals in the oil to be separated and identified. The oven temperature was set from 40 to 280 °C at a heating rate of 5 °C min^{-1}. The chromatograms were integrated, and the relative peak areas were calculated. These peaks were identified using the National Institute of Standards & Technology (NIST) library as a reference and only those with a matching quality of over 80% were taken into consideration. The FGA used a 1/8″ packed column and a thermal conductivity detector to analyse the gases produced during fast pyrolysis that were not easily assayed using capillary GC/MS. The absorbent trap of the pyrolizer collected the organic products from pyrolysis and transferred them to the GC/MS as usual. All analyses were carried out in triplicates to ensure reproducibility.

The peak area based on a Py-GC/MS and Py-FGA analysis could not reveal the real contents of the target compounds. However, if the sample masses matched in each fast pyrolysis experiment, the corresponding chromatographs could be compared to reveal the proportions and selectivities of the components in the oils.

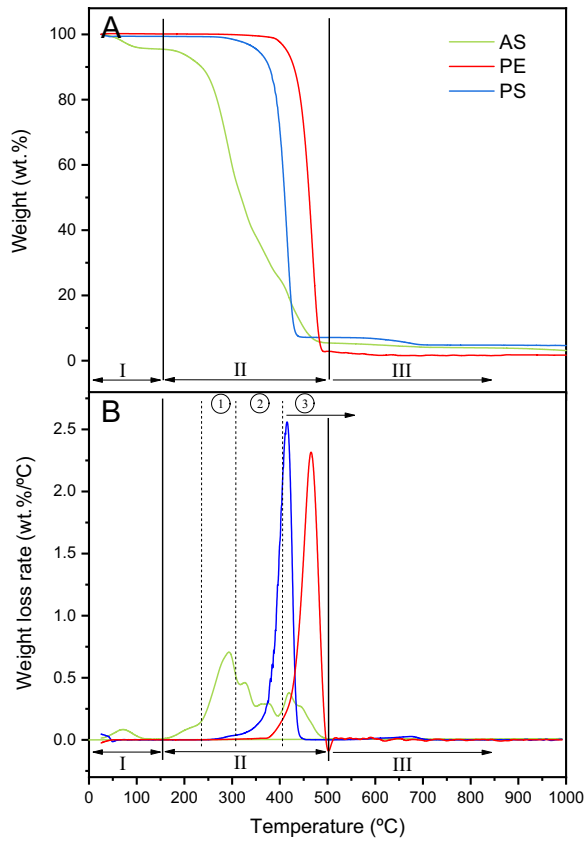

Fig. 1 Thermogravimetric analysis: **A** TG and **B** DTG curves for raw feedstocks

Results and discussion

Characterization of feedstock materials

The physicochemical properties of the materials used herein can be found in Table 1. From the proximate analysis, almond shell biomass contained the most fixed carbon in comparison to polyolefins (PE and PS). These plastic wastes were fundamentally formed by volatile matter, which indicates they may be good materials to be pyrolyzed [31]. However, these materials contained the highest amount of carbon: 85.7 and 92.3 wt% for PE and PS, respectively. Both plastic feeds gave a greater HHV, which was 41 MJ/kg, similar to that in commercial fuels such as gasoline and diesel [32]. Alkali and alkaline earth metals (AAEMs) content (mineral content in Table 1) were a key factor to consider, as they can act as indigenous catalysts in fast pyrolysis and in this way can alter the final composition of the oil [33]. Potassium, with 1.16 wt%, was the most abundant metal. Regarding the

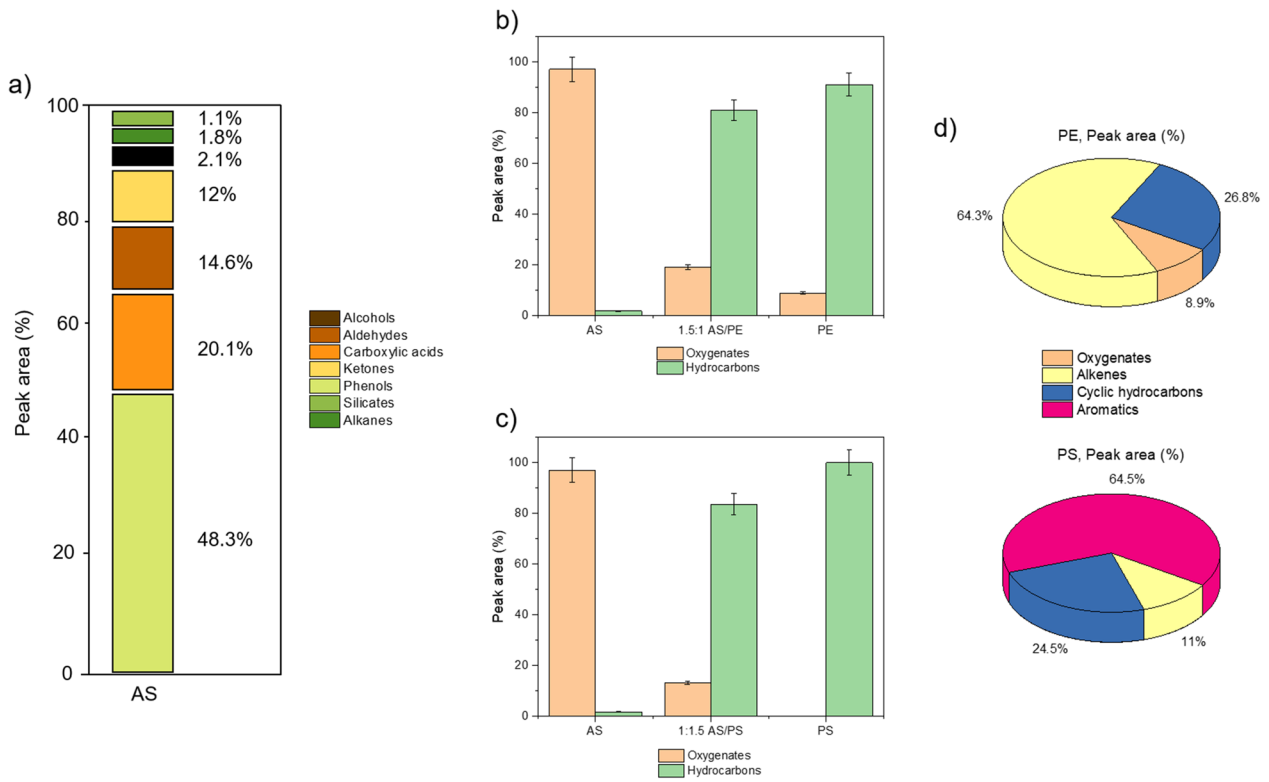

Fig. 2 Bio-oil product yield obtained from fast pyrolysis of **a** AS, **b** AS and PE blends, **c** AS and PS blends and **d** raw PE and PS

chemical composition, hemicellulose was the main fraction obtained with AS, as expected [34].

The effective hydrogen-to-carbon molar ratio (H/C_{eff}) in Table 1, shows the potential of the feed to be converted economically into hydrocarbons. Moreover, it enabled overall yields of olefin and aromatic compounds [35] to be estimated. The H/C_{eff} ratio for petroleum-derived feedstocks was between 1 and 2 and that for lignocellulosic biomass was between 0 and 0.3 [30, 36, 37]. The ratios for our feed lay within the same range. However, a catalyst is important for converting rich oxygen waste biomass (with a H/C_{eff} ratio under 1) into valuable hydrocarbons [38].

Thermal performance with the raw materials under an inert atmosphere was determined by thermogravimetric tests. The results, and the corresponding DTG curves, are shown in Fig. 1.

The main pyrolysis degradation step for AS took place at temperatures between 120 and 450 °C. However, pyrolysis was broken down into three common degradation stages: water drying/evaporation (stage I: 0–150 °C), devolatilization (stage II: 150–500 °C) and char formation (stage III: > 500 °C) [39]. The slight peak observed on the AS DTG curve at stage I reveals that the remaining moisture content of the sample was removed. At stage II, the DTG curve for AS displayed three clear shoulders: peak 1 was mainly attributed to the thermal decomposition of hemicellulose (250–340 °C), while peak 2 was largely due to cellulose decomposition (340–450 °C). Finally, peak 3 was attributed to lignin decomposition at higher temperatures (400–550 °C). This indicated that lignin had greater thermal stability compared to hemicellulose and cellulose due to its highly cross-linked structure. These results closely matched the chemical composition of AS (Table 1). Stage III was related to the carbonization of the biomass sample. Furthermore, the thermogravimetric analysis revealed the thermal stability of AS was lower than that for the plastics during pyrolysis. PE degraded at a higher temperature range (410–520 °C) as did PS (350 to 440 °C, while remaining components degraded in the temperature range of 440–550 °C [40]). In general, most synthetic polymers (such as PE and PS) thermally decomposed by random scission and radical mechanisms: initiation, propagation and termination [30, 41]. The carbon-to-hydrogen (C–H) bonds in primary, secondary and tertiary carbon atoms, and the carbon-to-carbon (C–C) sigma bond are the only ones that makes probability distribution in bonds selected from radical formation or breakage [42]. However, from straight chain polymers

hydrogen gas and hydrocarbon compounds were formed from straight chain polymers [8].

According to the TG/DTG results, AS was less thermally instable than plastics (PE and PS). Furthermore, those polymers could provide hydrogen, a chemical element which AS lacked, due to the range of fast pyrolysis temperatures used.

Bio-oil distribution of almond shell and plastic waste blends

The fast pyrolysis product distribution for AS and the blends with PE and PS is shown in Fig. 2. Firstly, almond shell was pyrolyzed at 650 °C to observe how oxygenated products were distributed. The compounds detected were separated into functional groups of alcohols, aldehydes, carboxylic acids, ketones, phenols, silicates and alkanes, as shown in Fig. 2a. Phenols, with yields of up to 48.3% and which mostly came from lignin decomposition [39] were the main groups detected. However, the inherent AAEMs in samples, such as K (1.16 wt%), helped phenolic compounds to form [43]. Carboxylic acids, whose yields came to 20.1%, were one of the main products obtained. According to the literature, such a high yield of acids may be explained by the fact the raw biomass was rich in hemicellulose (Table 1) which underwent ring scission to produce the acid [44]. Silicates with the bio-oil distribution could be observed after fast pyrolysis of AS and this might have been due to soil contamination, from gathering the biomass, transportation or transformation [26, 45]. In addition, nut shells generally contain some amounts of silicon in its chemical structure [46, 47].

Fast pyrolysis PE product distribution was mainly based on hydrocarbons in which alkanes, whose yield was 64.2%, were the main group. Most olefins observed were in the C_{11}–C_{20} carbon range and accounted for 49% of the total condensable compounds. Singh et al. [40] have also reported that the pyrolytic oil obtained from LDPE is producing a fraction of 21.30% and 67.76% in the carbon range of C_6–C_{12} and C_{13}–C_{22}, respectively. Other hydrocarbons found were cyclic hydrocarbons: 26.5% of cycloalkanes and 0.4% of cycloalkenes. As for the product distribution for the fast pyrolysis of PS, solely hydrocarbons were produced, whose yields of olefins, cyclic hydrocarbons and aromatic compounds came to 11%, 24.4% and 64.54%, respectively. As expected from aromatics, styrene was largely detected as main compositional monomer of PS [48, 49]. Among detected aromatics, benzene and toluene were obtained with yields of 2.5% and 8.8%, respectively.

PE reduced the amount of oxygen in the blend with AS, whereas carbon yields increased. This is because PE had a higher HHV than the biomass waste (Table 1). However, as expected, a synergistic effect was obtained for blends of AS/PE in fast pyrolysis (Fig. 2b) and reflected by higher amounts of hydrocarbons. Yields of hydrocarbons, all of which were alkanes, increased to 81.1%. Synergy was positive to produce aliphatic compounds and negative to produce aromatic compounds [13]. Aliphatic compound yields were distributed as follows: 27.2% for light olefins (C_6–C_{11}) and 53.9% for long chain olefins (C_{11}–C_{20}). In short, the AS and PE blends altered the reaction mechanisms, removing oxygenates by substituting decarbonylation and decarboxylation with dehydration [42]. This synergy could have been due to hydrogen abstraction of AS oxygenates and reactive radicals, which helped PE to degrade and boosted yields of aliphatic hydrocarbons [50, 51].

Regarding Fig. 2c, in the AS/PS blend there were higher yields of hydrocarbons in comparison to pure AS. Here, the relative content of hydrocarbons accounted for 83.7% of carbon yields, in which 44.2% of the condensable compounds detected were aromatics. Nonetheless, all these components were monocyclic aromatic compounds (MAHs), and not valuable hydrocarbons such as BTX. The pyrolytic environment of biomass and PS favoured alkylated benzene generation due to the interactions of PS-derived aromatics [17]. Reshad et al. conducted a study on the production of pyrolytic oil and char from a blend of seed cake and waste PS and found that the production of aromatic compounds increased with a higher proportion of PS in the mixture [52]. Van Nguyen et al. demonstrated that the water content and acetic acid concentration of bio-crude oil from co-pyrolysis of pine sawdust and PS decreased almost proportionally with the increasing PS ratio. Moreover, the production of hydrocarbon compounds increased, indicating that a synergistic effect was achieved during co-pyrolysis [15]. These findings are consistent with previous works, which have shown that adding PS to lignocellulosic biomass blends can improve the quality of the oil by transforming oxygenated compounds into aromatics.

Catalytic fast pyrolysis of almond shell and polyethylene blend (AS/PE)

Product yields from the catalytic fast co-pyrolysis of AS in the PE blend are shown in Fig. 3. Here, plastic was expected to reduce oxygen at the organic phase whilst carbon yield increased which resulted in a higher calorific value [53]. The components observed in the oil were split into two groups: hydrocarbons and oxygenates. Hydrocarbons were mainly composed of olefins, cyclic hydrocarbons and aromatics. These, in turn, were split into monocyclic aromatic hydrocarbons (MAHs), mainly benzenes rings; and polycyclic aromatic hydrocarbons (PAHs), categorized as naphthalene and its derivatives,

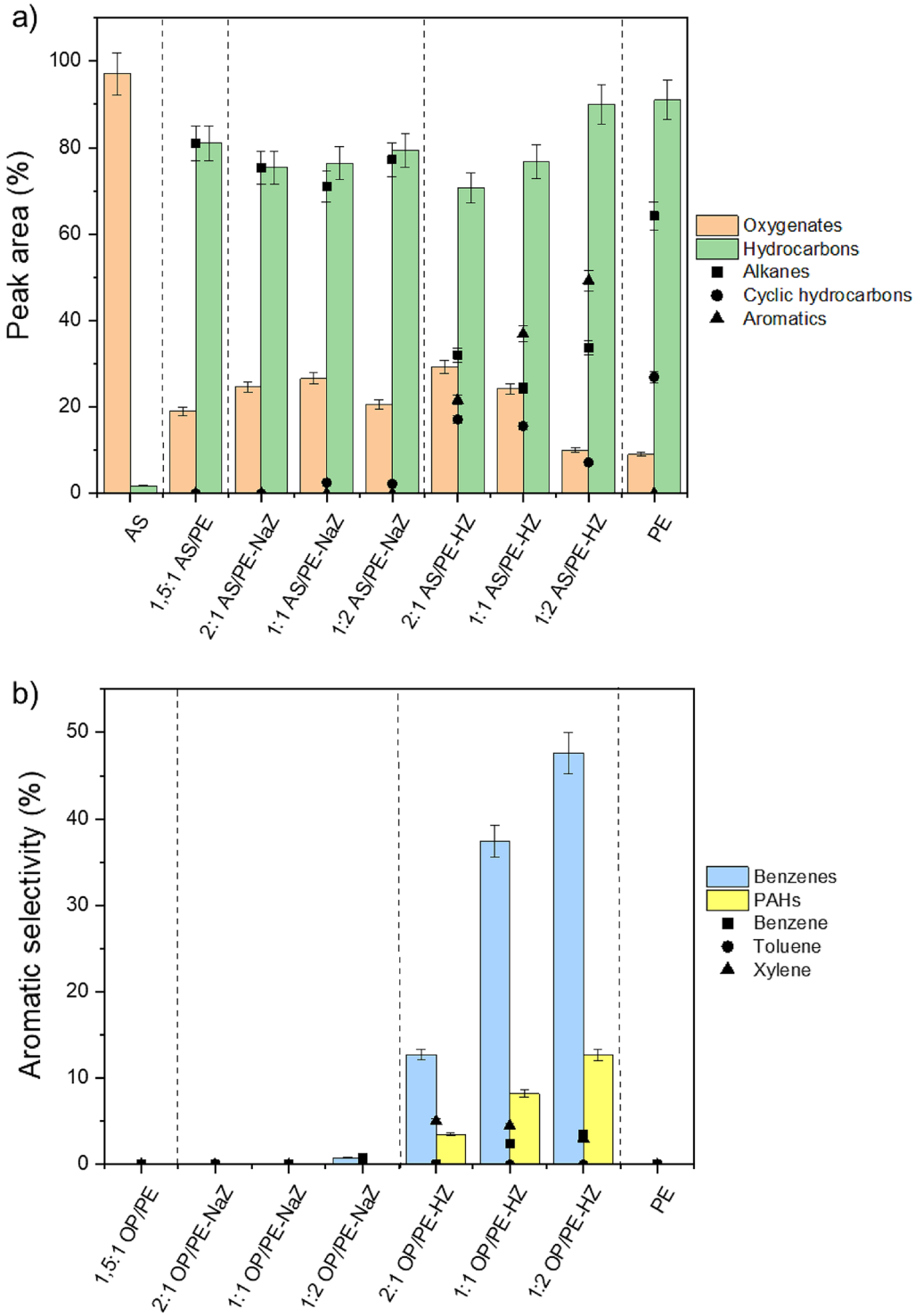

Fig. 3 **a** Bio-oil catalytic fast co-pyrolysis and **b** aromatic selectivity of 1.5:1 AS/PE over NaZSM-5 (AS/PE-NaZ) and HZSM-5 (AS/PE-HZ) zeolites

indene and its derivatives, and multi-ring aromatic components with over two rings. In addition, oxygenates were produced from alcohols, aldehydes, carboxylic acids, esters, ketones and phenols.

Aliphatic hydrocarbons derived from the pyrolysis of PE could interact with the oxygenated fraction in AS by cracking, cyclization and isomerization. This increased hydrocarbon diversity (alkenes and cyclic hydrocarbons)

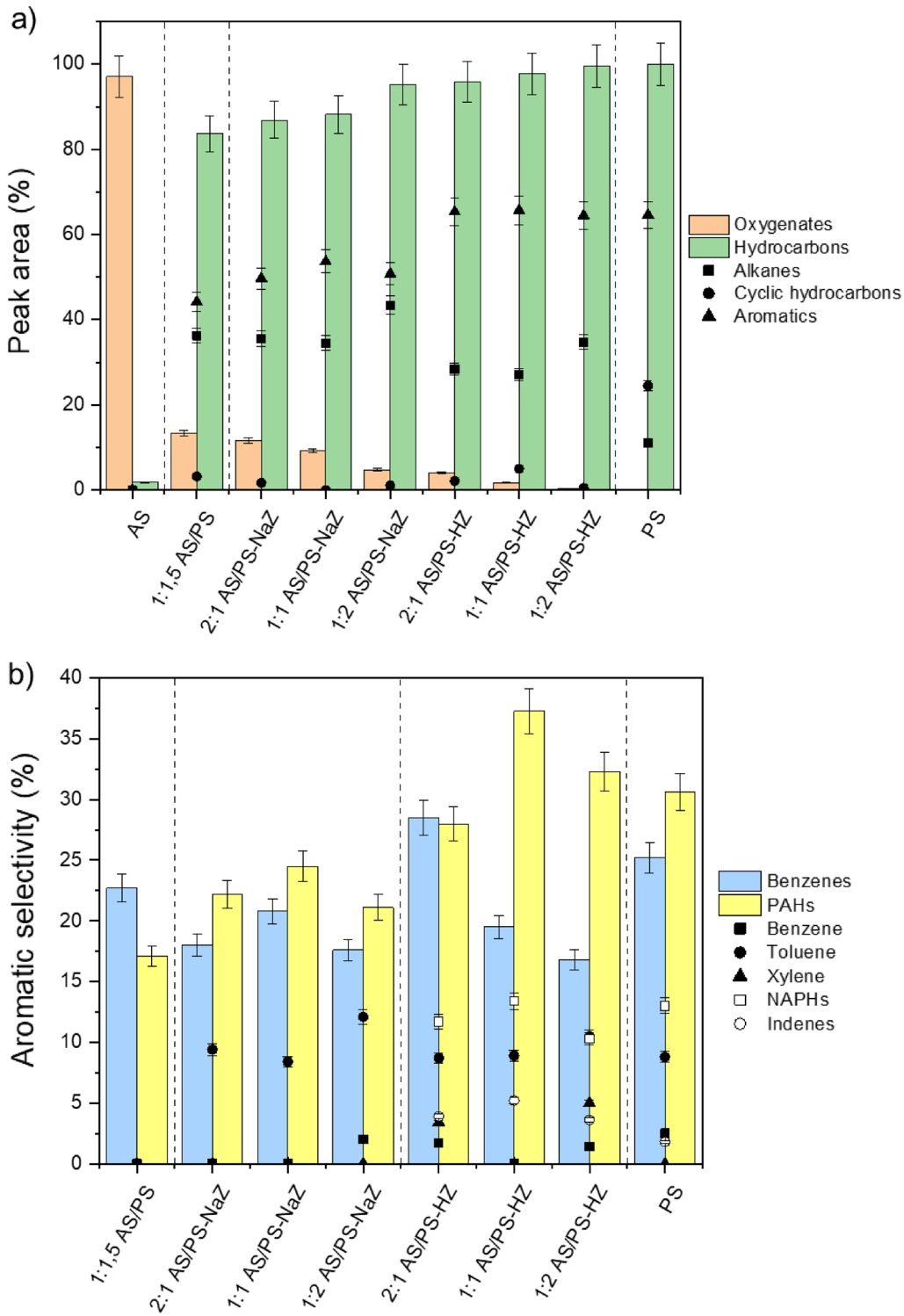

Fig. 4 **a** Bio-oil catalytic fast co-pyrolysis and **b** aromatic selectivity of 1:1.5 AS/PS over NaZSM-5 (AS/PS-NaZ) and HZSM-5 (AS/PS-HZ) zeolites

[42]. Without a catalyst, approximately 80% of that produced from 1.5:1 AS/PE was hydrocarbon compounds, most of which were aliphatic in the C_6–C_{20} range. On adding NaZSM-5 (NaZ), the amount of hydrocarbon compounds fell, and oxygenated products increased slightly from 18.9 to 26.6% for pure AS and 1:2 AS/PE-NaZ. This led to an increase in phenolics and acids fractions. This could be attributed to the catalytic effect of

inherent metals (AAEMs) and the additional sodium in the NaZ zeolite, which hindered the formation of hydrocarbons. The extra Na^+ in the blend promoted cracking and dehydration, which favoured the formation of light compounds such as carboxylic acids [26, 54]. As shown in Fig. 3a, an increase in NaZ content did not have significant effects on aromatic production, consistent with the findings of Ghorbannezhad et al., who investigated the effects of sodium-based catalysts on co-pyrolysis [55]. The only hydrocarbons detected were olefins C_6–C_{20}, and more than half of these were in the C_7–C_{10} range.

After adding HZSM-5 (HZ), the amount of hydrocarbons increased in a wide range of compounds. Yields in AS/PE blends increased from 70.7 to 90% as the amount of HZ in the blend increased. Furthermore, the total percentage of hydrocarbons also increased in comparison to the blends without a catalyst, as, HZ clearly enhanced production of aromatics. In Fig. 3a, it was observed that aromatic selectivity increased at the expense of the proportion of aliphatic compounds. Aromatics were the main product (accounting for over 45% of total hydrocarbons) for 1:2 AS/PE-HZ. Results revealed that yields of xylene were 2.1% (2:1 AS/PE-HZ) and 1.4% (1:2 AS/PE-HZ). Dorado et al. observed for switchgrass and PE blends in presence of HZSM-5 yielded less toluene than would be predicted for the non-interacting blend. However, these blends show increases over the predicted values of the blends for *p*-xylene and ethylbenzene. This indicates that the change in selectivity in the conversion to aromatics for cellulose in the presence of the PE is the opposite of what is observed for lignin [56]. As shown in Fig. 3b, the sum of benzene compounds was higher than that of PAHs compounds (an undesirable group) [30, 49].

Catalytic fast pyrolysis of almond shell and polystyrene blend (AS/PS)

The effect of zeolites (NaZSM-5 and HZSM-5) in AS/PS blends on bio-oil product distribution is shown in Fig. 4. The composition of the oil from the fast pyrolysis of PS was oxygen-free. In comparison to PE, PS is low in aliphatics due to the aromatic nature of the styrene monomer [15]. The general catalytic effect on the 1:1.5 AS/PS blend was to increase yields of aromatics, in which toluene was enhanced in comparison to the pure feedstock. On adding NaZSM-5, toluene yields increased to 12% for 1:2 AS/PS-NaZ. It was reported that the metal-modified ZSM-5 catalysts increased oil yield and single-ring aromatic content of the product oil compared to unmodified HZSM-5 catalyst, like toluene. The consequence is a reduction in the rate of catalyst coke formation and thereby improved hydrocarbon yield. The addition of metals to ZSM-5 zeolite is also reported to be selective towards the formation of increased single-ring aromatic compounds [23]. The catalytic effect of Na tended to be higher due to the sum of the sodium inherent in AS and that added from NaZSM-5. The AAEMs altered the co-pyrolysis intermediates by increasing yields of mono-aromatics while PAHs fell. They could promote intermolecular and intramolecular dehydration, protonation, and aromatization. With HZSM-5 hydrocarbon yields increased in the blend to nearly 100% of total condensable compounds. HZSM-5 acted as a catalyst which enhanced production of aromatics in the AS/PS blend, in which the main group detected was aromatics. As cited above, toluene production was enhanced greatly, followed by benzene and 1,3,5-cycloheptatriene for cyclic hydrocarbons. Here, more PAHs than MAHs were obtained, as observed in Fig. 4b. A large amount of naphthalene was obtained from the PAHs in 1:2 AS/PS-HZ, which accounted for 3.4% of aromatic yields. The fraction of naphthalene derivates (NAPHs) increased with the higher presence of HZ in the AS/PS blends (as shown in Fig. 4b, it accounted yields of 11.7, 13.3 and 10.3% for 2:1 AS/PS-HZ, 1:1 AS/PS-HZ and 1:2 AS/PS-HZ, respectively). The same was true for indenes which reached yields of 3.9, 5.2 and 3.6% for AS, PS and HZ, respectively. As expected, vapours from co-pyrolysis of AS/PS diffused into the pores of HZSM-5 and underwent deoxygenation, isomerization, and oligomerization at the acid sites in order to form aromatics [57].

Conclusions

Results showed that zeolites acted as a catalyst in the co-pyrolysis of AS/PE and AS/PS blends to enhance hydrocarbon selectivity. The oil yielded from AS was mainly formed by oxygenated components, with phenolics amounting to 48.3%. For the AS/PE blends hydrocarbons, all of which were alkanes, increased to 81.1%. Aliphatic compounds were distributed in 27.2% of light olefins (C_6–C_{11}) and yields of long chain olefins (C_{11}–C_{20}) amounted to 53.9%. For AS/PS, more hydrocarbons were produced than in pure AS (83.7%). As for the zeolite catalytic effect, it was found that NaZ in blends with PE enhanced alkene production. In general, hydrocarbon selectivity was greatly enhanced after adding HZSM-5 zeolite. For AS/PE blends, this increase from 70.7 to 90%, resulted in a rapid change in aromatics, being up to 45% of total hydrocarbons for 1:2 AS/PE-HZ. In general, it was observed that in the case of AS/PE-HZ blends, the production of MAHs was higher compared to PAHs (38.7% and 9.2%, respectively), and there was a reduction in the production of cyclic hydrocarbons. On the other hand, in the case of AS/PS-HZ

blends, the hydrocarbon yield was nearly 100% of total condensable compounds, and it was observed that HZ had no significant effect on the aromatic content. In this study, plastics were used as a source of hydrogen-rich material in co-pyrolysis with biomass. This is one way of reducing waste from plastic. In conclusion, catalytic co-pyrolysis of AS and plastics was found as a promising solution to improve bio-oil composition.

Acknowledgements
Not applicable.

Author contributions
AA-R, LS-S and FD contributed to the study conception and design. Material preparation, data collection and analysis were performed by AA-R. The first draft of the manuscript was written by AA-R. LS-S and FD supervised all the versions of the manuscript.

Funding
The authors declare that no funds, grants, or other support were received during the preparation of this manuscript.

Availability of data and materials
The datasets generated during and/or analysed during the current study are available from the corresponding author on reasonable request.

Declarations

Ethics approval and consent to participate
Not applicable.

Consent for publication
All authors listed have read the complete manuscript and have approved submission of the paper.

Competing interests
The authors have no relevant financial or non-financial interests to disclose.

Author details
[1]Department of Chemical Engineering, University of Castilla-La Mancha, Avda. Camilo José Cela 12, 13071 Ciudad Real, Spain.

Received: 6 March 2023 Accepted: 15 June 2023
Published online: 26 June 2023

References

1. Vo TA, Tran QK, Ly HV, Kwon B, Hwang HT, Kim J, Kim SS. Co-pyrolysis of lignocellulosic biomass and plastics: a comprehensive study on pyrolysis kinetics and characteristics. J Anal Appl Pyrolysis. 2022;163: 105464. https://doi.org/10.1016/j.jaap.2022.105464.
2. Debevc S, Weldekidan H, Snowdon MR, Vivekanandhan S, Wood DF, Misra M, Mohanty AK. Valorization of almond shell biomass to biocarbon materials: influence of pyrolysis temperature on their physicochemical properties and electrical conductivity. Carbon Trends. 2022;9: 100214. https://doi.org/10.1016/J.CARTRE.2022.100214.
3. González JF, Ramiro A, González-García CM, Gańán J, Encinar JM, Sabio E, Rubiales J. Pyrolysis of almond shells. Energy applications of fractions. Ind Eng Chem Res. 2005;44:3003–12. https://doi.org/10.1021/ie0490942.
4. NUTFRUIT—Plant-based power—INC (n.d.). https://www.nutfruit.org/. Accessed 22 Nov 2022.
5. Dorado F, Sanchez P, Alcazar-Ruiz A, Sanchez-Silva L. Fast pyrolysis as an alternative to the valorization of olive mill wastes. J Sci Food Agric. 2020. https://doi.org/10.1002/jsfa.10856.
6. Fonseca FG, Soares Dias AP. Almond shells: catalytic fixed-bed pyrolysis and volatilization kinetics. Renew Energy. 2021;180:1380–90. https://doi.org/10.1016/J.RENENE.2021.08.104.
7. Sánchez E, Zabaleta R, Fabani MP, Rodriguez R, Mazza G. Effects of the amendment with almond shell, bio-waste and almond shell-based biochar on the quality of saline-alkali soils. J Environ Manag. 2022;318: 115604. https://doi.org/10.1016/J.JENVMAN.2022.115604.
8. Salvilla JNV, Ofrasio BIG, Rollon AP, Manegdeg FG, Abarca RRM, de Luna MDG. Synergistic co-pyrolysıs of polyolefin plastics with wood and agricultural wastes for biofuel production. Appl Energy. 2020;279: 115668. https://doi.org/10.1016/j.apenergy.2020.115668.
9. Xiao J, Yang M, Che Q, Chen Y, Chen X, Yang H, Bartocci P, Fantozzi F, Chen H. Effect of potassium on catalytic characteristics of ZSM-5 zeolite in fast pyrolysis of biomass-based furan. J Anal Appl Pyrolysis. 2021;157: 105230. https://doi.org/10.1016/J.JAAP.2021.105230.
10. Wang W, Luo G, Zhao Y, Tang Y, Wang K, Li X, Xu Y. Kinetic and thermodynamic analyses of co-pyrolysis of pine wood and polyethylene plastic based on Fraser-Suzuki deconvolution procedure. Fuel. 2022;322: 124200. https://doi.org/10.1016/j.fuel.2022.124200.
11. Sun J, Luo J, Lin J, Ma R, Sun S, Fang L, Li H. Study of co-pyrolysis endpoint and product conversion of plastic and biomass using microwave thermogravimetric technology. Energy. 2022;247: 123547. https://doi.org/10.1016/j.energy.2022.123547.
12. Parthasarathy P, Narayanan SK. Effect of hydrothermal carbonization reaction parameters on. Environ Prog Sustain Energy. 2014;33:676–80. https://doi.org/10.1002/ep.11974.
13. Yang J, Rizkiana J, Widayatno WB, Karnjanakom S, Kaewpanha M, Hao X, Abudula A, Guan G. Fast co-pyrolysis of low density polyethylene and biomass residue for oil production. Energy Convers Manag. 2016;120:422–9. https://doi.org/10.1016/J.ENCONMAN.2016.05.008.
14. Al-Maari MA, Ahmad MA, Din ATM, Hassan H, Alsobaai AM. Co-pyrolysis of oil palm empty fruit bunch and oil palm frond with low-density polyethylene and polypropylene for bio-oil production. Arab J Chem. 2021;14: 103282. https://doi.org/10.1016/j.arabjc.2021.103282.
15. Van Nguyen Q, Choi YS, Choi SK, Jeong YW, Kwon YS. Improvement of bio-crude oil properties via co-pyrolysis of pine sawdust and waste polystyrene foam. J Environ Manag. 2019;237:24–9. https://doi.org/10.1016/j.jenvman.2019.02.039.
16. Gin AW, Hassan H, Ahmad MA, Hameed BH, Mohd Din AT. Recent progress on catalytic co-pyrolysis of plastic waste and lignocellulosic biomass to liquid fuel: the influence of technical and reaction kinetic parameters. Arab J Chem. 2021;14: 103035. https://doi.org/10.1016/j.arabjc.2021.103035.
17. Ansari KB, Hassan SZ, Bhoi R, Ahmad E. Co-pyrolysis of biomass and plastic wastes: a review on reactants synergy, catalyst impact, process parameter, hydrocarbon fuel potential, COVID-19. J Environ Chem Eng. 2021;9: 106436. https://doi.org/10.1016/J.JECE.2021.106436.
18. Cai R, Pei X, Pan H, Wan K, Chen H, Zhang Z, Zhang Y. Biomass catalytic pyrolysis over zeolite catalysts with an emphasis on porosity and acidity: a state-of-the-art review. Energy Fuels. 2020;34:11771–90.
19. Chaihad N, Anniwaer A, Choirun Az Zahra A, Kasai Y, Reubroycharoen P, Kusakabe K, Abudula A, Guan G. In-situ catalytic upgrading of bio-oil from rapid pyrolysis of biomass over hollow HZSM-5 with mesoporous shell. Bioresour Technol. 2021;341: 125874. https://doi.org/10.1016/j.biortech.2021.125874.
20. Wei B, Jin L, Wang D, Xiong Y, Hu H, Bai Z. Effect of different acid-leached USY zeolites on in-situ catalytic upgrading of lignite tar. Fuel. 2020;266: 117089.
21. Lazaridis PA, Fotopoulos AP, Karakoulia SA, Triantafyllidis KS. Catalytic fast pyrolysis of kraft lignin with conventional, mesoporous and nanosized ZSM-5 zeolite for the production of alkyl-phenols and aromatics. Front Chem. 2018;6:295. https://doi.org/10.3389/fchem.2018.00295.
22. Lin X, Zhang D, Ren X, Zhang Q, Cai H, Yi W, Lei H. Catalytic co-pyrolysis of waste corn stover and high-density polyethylene for hydrocarbon production: the coupling effect of potassium and HZSM-5 zeolite. J Anal Appl Pyrolysis. 2020;150: 104895. https://doi.org/10.1016/j.jaap.2020.104895.
23. Dyer AC, Nahil MA, Williams PT. Biomass: polystyrene co-pyrolysis coupled with metal-modified zeolite catalysis for liquid fuel and chemical production. J Mater Cycles Waste Manag. 2022;24:477–90. https://doi.org/10.1007/s10163-021-01334-0.

24. Xu D, Guo S, Liu L, Hua H, Guo Y, Wang S, Jing Z. Ni-Ru/CeO_2 catalytic hydrothermal upgrading of water-insoluble biocrude from algae hydrothermal liquefaction. Biomed Res Int. 2018. https://doi.org/10.1155/2018/8376127.
25. Alcazar-Ruiz A, Sanchez-Silva L, Dorado F. Enhancement of BTX production via catalytic fast pyrolysis of almond shell, olive pomace with polyvinyl chloride mixtures. Process Saf Environ Prot. 2022;163:218–26. https://doi.org/10.1016/J.PSEP.2022.05.029.
26. Alcazar-Ruiz A, Ortiz ML, Sanchez-Silva L, Dorado F. Catalytic effect of alkali and alkaline earth metals on fast pyrolysis pre-treatment of agricultural waste. Biofuels Bioprod Biorefining. 2021;15:1–12. https://doi.org/10.1002/bbb.2253.
27. López-González D, Fernandez-Lopez M, Valverde JL, Sanchez-Silva L. Thermogravimetric-mass spectrometric analysis on combustion of lignocellulosic biomass. Bioresour Technol. 2013;143:562–74. https://doi.org/10.1016/J.BIORTECH.2013.06.052.
28. TAPPI, TAPPI/ANSI test method T 401 om-15—fiber analysis of paper and paperboard; 2018.
29. Dorado F, Romero R, Cañizares P. Influence of clay binders on the performance of Pd/HZSM-5 catalysts for the hydroisomerization of n-butane. Ind Eng Chem Res. 2001;40:3428–34. https://doi.org/10.1021/ie001133w.
30. Alcazar-Ruiz A, Dorado F, Sanchez-Silva L. Fast pyrolysis of agroindustrial wastes blends: hydrocarbon production enhancement. J Anal Appl Pyrolysis. 2021;157: 105242. https://doi.org/10.1016/j.jaap.2021.105242.
31. Braga RM, Melo DMA, Melo MAF, Freitas JCO, Boateng AA. Effect of pretreatment on pyrolysis products of *Pennisetum purpureum* Schum. by Py-GC/MS. J Therm Anal Calorim. 2021. https://doi.org/10.1007/s10973-021-11025-5.
32. Perkins G, Bhaskar T, Konarova M. Process development status of fast pyrolysis technologies for the manufacture of renewable transport fuels from biomass. Renew Sustain Energy Rev. 2018;90:292–315. https://doi.org/10.1016/j.rser.2018.03.048.
33. Fermoso J, Hernando H, Jiménez-Sánchez S, Lappas AA, Heracleous E, Pizarro P, Coronado JM, Serrano DP. Bio-oil production by lignocellulose fast-pyrolysis: isolating and comparing the effects of indigenous versus external catalysts. Fuel Process Technol. 2017;167:563–74. https://doi.org/10.1016/j.fuproc.2017.08.009.
34. Schmitt CC, Moreira R, Neves RC, Richter D, Funke A, Raffelt K, Grunwaldt J-D, Dahmen N. From agriculture residue to upgraded product: the thermochemical conversion of sugarcane bagasse for fuel and chemical products. Fuel Process Technol. 2020;197: 106199. https://doi.org/10.1016/J.FUPROC.2019.106199.
35. Wang Z, Burra KG, Lei T, Gupta AK. Co-pyrolysis of waste plastic and solid biomass for synergistic production of biofuels and chemicals—a review. Prog Energy Combust Sci. 2021;84: 100899. https://doi.org/10.1016/j.pecs.2020.100899.
36. Zhang H, Cheng YT, Vispute TP, Xiao R, Huber GW. Catalytic conversion of biomass-derived feedstocks into olefins and aromatics with ZSM-5: the hydrogen to carbon effective ratio. Energy Environ Sci. 2011;4:2297–307. https://doi.org/10.1039/c1ee01230d.
37. Huang Y, Qiu S, Oduro IN, Guo X, Fang Y. Production of high-yield bio-oil with a high effective hydrogen/carbon molar ratio through acidolysis and in situ hydrogenation. Energy Fuels. 2016;30:9524–31. https://doi.org/10.1021/acs.energyfuels.6b02250.
38. Chen NY, Degnan TF, Koenig LR. Liquid fuel from carbohydrates. ChemTech. 1986;16:506–11.
39. Puig-Gamero M, Alcazar-Ruiz Á, Sánchez P, Sanchez-Silva L. Binary blends versus ternary blends in steam cogasification by means of TGA–MS: reactivity and H_2/CO ratio. Ind Eng Chem Res. 2020. https://doi.org/10.1021/acs.iecr.0c01399.
40. Singh RK, Ruj B, Sadhukhan AK, Gupta P. Impact of fast and slow pyrolysis on the degradation of mixed plastic waste: product yield analysis and their characterization. J Energy Inst. 2019;92:1647–57. https://doi.org/10.1016/j.joei.2019.01.009.
41. Wu F, Ben H, Yang Y, Jia H, Wang R, Han G. Effects of different conditions on co-pyrolysis behavior of corn stover and polypropylene. Polymers (Basel). 2020;12:973. https://doi.org/10.3390/POLYM12040973.
42. Zhang X, Lei H, Chen S, Wu J. Catalytic co-pyrolysis of lignocellulosic biomass with polymers: a critical review. Green Chem. 2016;18:4145–69. https://doi.org/10.1039/c6gc00911e.
43. Alcazar-Ruiz A, Garcia-Carpintero R, Dorado F, Sanchez-Silva L. Valorization of olive oil industry subproducts: ash and olive pomace fast pyrolysis. Food Bioprod Process. 2021;125:37–45. https://doi.org/10.1016/j.fbp.2020.10.011.
44. Chen X, Che Q, Li S, Liu Z, Yang H, Chen Y, Wang X, Shao J, Chen H. Recent developments in lignocellulosic biomass catalytic fast pyrolysis: strategies for the optimization of bio-oil quality and yield. Fuel Process Technol. 2019;196: 106180. https://doi.org/10.1016/j.fuproc.2019.106180.
45. Green SK, Patet RE, Nikbin N, Williams CL, Chang CC, Yu J, Gorte RJ, Caratzoulas S, Fan W, Vlachos DG, Dauenhauer PJ. Diels-Alder cycloaddition of 2-methylfuran and ethylene for renewable toluene. Appl Catal B Environ. 2016;180:487–96. https://doi.org/10.1016/j.apcatb.2015.06.044.
46. Li X, Liu Y, Hao J, Wang W. Study of almond shell characteristics. Materials (Basel). 2018;11:1782. https://doi.org/10.3390/ma11091782.
47. Boulika H, El Hajam M. Physico-chemical proprieties of Almond residues (Shells & hulls) collected from the northern region of Morocco (Fez-Meknes). 2022. https://doi.org/10.21203/rs.3.rs-1676689/v1.
48. Zhang Z, Hirose T, Nishio S, Morioka Y, Azuma N, Ueno A, Ohkita H, Okada M. Chemical recycling of waste polystyrene into styrene over solid acids and bases. Ind Eng Chem Res. 1995;34:4514–9. https://doi.org/10.1021/ie00039a044.
49. Praveen Kumar K, Srinivas S. Catalytic co-pyrolysis of biomass and plastics (polypropylene and polystyrene) using spent FCC catalyst. Energy Fuels. 2020;34:460–73. https://doi.org/10.1021/acs.energyfuels.9b03135.
50. Li J, Yu Y, Li X, Wang W, Yu G, Deng S, Huang J, Wang B, Wang Y. Maximizing carbon efficiency of petrochemical production from catalytic co-pyrolysis of biomass and plastics using gallium-containing MFI zeolites. Appl Catal B Environ. 2015;172–173:154–64. https://doi.org/10.1016/j.apcatb.2015.02.015.
51. Dorado C, Mullen CA, Boateng AA. Origin of carbon in aromatic and olefin products derived from HZSM-5 catalyzed co-pyrolysis of cellulose and plastics via isotopic labeling. Appl Catal B Environ. 2015;162:338–45. https://doi.org/10.1016/j.apcatb.2014.07.006.
52. Reshad AS, Tiwari P, Goud VV. Thermal and co-pyrolysis of rubber seed cake with waste polystyrene for bio-oil production. J Anal Appl Pyrolysis. 2019;139:333–43. https://doi.org/10.1016/j.jaap.2019.03.010.
53. Zheng A, Xia S, Cao F, Liu S, Yang X, Zhao Z, Tian Y, Li H. Directional valorization of eucalyptus waste into value-added chemicals by a novel two-staged controllable pyrolysis process. Chem Eng J. 2021;404: 127045. https://doi.org/10.1016/j.cej.2020.127045.
54. Zhao N, Li B-X. The effect of sodium chloride on the pyrolysis of rice husk. Appl Energy. 2016;178:346–52.
55. Ghorbannezhad P, Park S, Onwudili JA. Co-pyrolysis of biomass and plastic waste over zeolite- and sodium-based catalysts for enhanced yields of hydrocarbon products. Waste Manag. 2020;102:909–18. https://doi.org/10.1016/j.wasman.2019.12.006.
56. Dorado C, Mullen CA, Boateng AA. H-ZSM5 catalyzed co-pyrolysis of biomass and plastics. ACS Sustain Chem Eng. 2014;2:301–11. https://doi.org/10.1021/sc400354g.
57. Li Z, Zhong Z, Zhang B, Wang W, Seufitelli GVS, Resende FLP. Catalytic fast co-pyrolysis of waste greenhouse plastic films and rice husk using hierarchical micro-mesoporous composite molecular sieve. Waste Manag. 2020;102:561–8. https://doi.org/10.1016/j.wasman.2019.11.012.

Publisher's Note